Modeling the Effects of Matrix Shrinkage and Differential Swelling on Coalbed Methane Recovery and Carbon Sequestration

L. J. Pekot and S. R. Reeves, Advanced Resources International, Arlington, Virginia and Houston, Texas

ABSTRACT

Matrix shrinkage and swelling can cause profound changes in porosity and permeability of coalbed methane reservoirs during depletion or when under injection processes, with associated implications for primary or enhanced methane recovery. Two models that are used to describe these effects are discussed. The first was developed by Advanced Resources International (ARI) and published in 1990 by Sawyer, et al. The second model was published by Palmer and Mansoori in 1996. This paper shows that the two provide equivalent results for most applications. However, their differences in formulation cause each to have relative advantages and disadvantages under certain circumstances. Specifically, the former appears superior for undersaturated CBM reservoirs while the latter would be better for a case where matrix swelling is strongly disproportional to gas concentration. Since its presentation in 1996, the Palmer and Mansoori model has justifiably received much critical praise. However, the model developed by ARI for the *COMET* reservoir simulation program, in use since 1990, has significant advantages in certain settings. A review of data published by Levine in 1996 reveals that carbon dioxide causes a greater degree of coal matrix swelling compared to methane, even when measured on a unit of concentration basis. This effect is described in this paper as differential swelling. Differential swelling may have important consequences for enhanced coalbed methane and carbon sequestration projects. To handle the effects of differential swelling, an extension to the matrix shrinkage and swelling model used by the *COMET* simulator is presented and shown to replicate the data of Levine. Preliminary field results from a carbon dioxide injection project are also presented in support of the extended model.

INTRODUCTION

The maturation of coalbed methane production operations in some basins, and the emergence of injection schemes for enhanced coalbed methane (ECBM) and carbon sequestration (CSEQ) of greenhouse gasses, has led to renewed focus on behavior of coalbed reservoir properties under these conditions. A limited body of laboratory and

field data demonstrates that coal matrix shrinkage and the resulting change in cleat or fracture system porosity can have a profound effect on reservoir permeability and thus also on production performance.

Coal has been shown to shrink on desorption of gas and expand again upon readsorption [1]. Harpalani and Schraufnagel [2] first demonstrated the impact on permeability that shrinkage had on a coal from the United States. This provided the impetus for Advanced Resources International (ARI) to develop a coal matrix shrinkage and permeability model that could be included in reservoir simulation software. That shrinkage model was developed for the *COMET* simulator and was published by Sawyer, et al. [3] in 1990. The ARI model uses gas concentration as an important parameter. Since 1990, other authors [4,5,6] have shown measured strain data that, when plotted versus pore pressure, produces a curve similar to the familiar gas sorption isotherm and can be described in terms of e_L and P_L, which are equivalent to the Langmuir isotherm volume and pressure parameters. In 1996 Palmer and Mansoori (P&M) published a shrinkage model that described matrix shrinkage more in terms of strain and the coal's rock mechanical properties [7]. P&M issued a revised edition of their publication in 1998 [8].

This paper compares the two shrinkage models and concludes that the two models provide equivalent results for the most common CBM reservoir conditions. However, different results can be expected for reservoirs that are undersaturated or have unusual swelling behavior.

Most available laboratory data, as might be expected, represents methane (CH_4) systems. The more limited data for carbon dioxide (CO_2) systems not only shows that CO_2 adsorption causes more strain and swelling than CH_4 because, on a unit of pressure basis, it is adsorbed in higher concentration by a coal, but also suggests that CO_2 causes more swelling on a unit of concentration basis. That is, 600 SCF/ton of CO_2 causes more swelling than 600 SCF/ton of CH_4. This differential swelling behavior has important consequences for field injection projects and the ability of industry to numerically model the process. Therefore, an extension to the ARI model is also presented that accounts for this behavior.

COMPARISON OF THEORETICAL MODELS

The ARI model, as presented by Sawyer et al., for the change of coal porosity due to pore compressibility, shrinkage and swelling is expressed as

$$\phi = \phi_i \left[1 + c_p(P-P_i)\right] - c_m \left(1 - \phi_i\right) \left(\frac{\Delta P_i}{\Delta C_i}\right) (C-C_i) \qquad (1)$$

The P&M model is presented as *

$$\frac{\phi}{\phi_i} = 1 + \frac{A_m}{\phi_i}(P - P_i) + \frac{\varepsilon_L}{\phi_i}\left(\frac{K}{M} - 1\right)\left(\frac{\beta P}{1+\beta P} - \frac{\beta P_i}{1+\beta P_i}\right) \quad (2)$$

Seidle and Huitt [4] write the following for bulk swelling if it is proportional to adsorbed gas concentration,

$$\varepsilon_m = S_m V_L \frac{\beta P}{1+\beta P} \quad (3)$$

where S_m is the matrix swelling coefficient with units of micro strain-ton / SCF and converts the Langmuir isotherm equation to provide the amount of matrix strain, which is dimensionless.

P&M [7] define ε_L as the Langmuir dimensionless volumetric strain constant. Assuming swelling is proportional to concentration,

$$\varepsilon_L = S_m V_L \quad (4)$$

and

$$\beta = \frac{1}{P_L} \quad (5)$$

Now, multiplying Equ.2 by ϕ_i, and substituting from Equs. 4 and 5 gives

$$\phi = \phi_i + A_m(P-P_i) + S_m V_L \left(\frac{K}{M} - 1\right)\left(\frac{(1/P_L)P}{1+(1/P_L)P} - \frac{(1/P_L)P_i}{1+(1/P_L)P_i}\right) \quad (6)$$

Rearranging,

$$\phi = \phi_i + A_m(P-P_i) + S_m\left(\frac{K}{M} - 1\right)\left(\frac{V_L P}{P_L + P} - \frac{V_L P_i}{P_L + P_i}\right) \quad (7)$$

since gas concentration , C, is calculated by the Langmuir formulation

* Minor changes to the original notation have been made since some references use the same nomenclature to define different parameters. This is especially true of the parameter c_m, which is defined in this paper as $1/V_m\,(\Delta V_m/\Delta P)$ and has the units of psi^{-1}. Reference No. 2 uses c'_m for the same definition. Reference No. 4 uses c_m to define a matrix swelling coefficient with units of microstrain-ton/SCF. Reference Nos. 7 and 8 also use c_m and define it in terms of elastic moduli but do not name it or describe its significance.

$$C = \frac{V_L P}{P_L + P} \tag{8}$$

then

$$\phi = \phi_i + A_m(P-P_i) + S_m\left(\frac{K}{M} - 1\right)(C - C_i) \tag{9}$$

P&M also define

$$A_m = \frac{1}{M} - \left[\frac{K}{M} + f\text{-}1\right]\gamma \tag{10}$$

and

$$c_p = \frac{1}{\phi}\frac{d\phi}{d} = \frac{1}{\phi M} \tag{11}$$

where grain compressibility, γ, is small and can be disregarded,

$$A_m = \frac{1}{M} = c_p\phi \tag{12}$$

substituting equ 13 into equ 10 yields

$$\phi = \phi_i + c_p\phi\,(P-P_i) + S_m\left(\frac{K}{M} - 1\right)(C - C_i) \tag{13}$$

As noted by P&M, this is very similar to the ARI model, equ. 1.

Equating equations 14 and 1

$$S_m\left(\frac{K}{M} - 1\right) = -c_m\left(1 - \phi_i\right)\frac{\Delta P_i}{\Delta C_i} \tag{14}$$

also from P&M

$$\frac{K}{M} = \frac{1}{3}\left(\frac{1+\upsilon}{1-\upsilon}\right) \tag{15}$$

and after rearranging equation 3 in terms of S_m, equations 3 and 15 can be substituted into equation 14 to create

$$\left[\frac{1}{3}\left(\frac{1+\upsilon}{1-\upsilon}\right) - 1\right]\varepsilon_m\left(\frac{P_L + P}{V_L P}\right) = -c_m\left(1 - \phi_i\right)\frac{\Delta P_i}{\Delta C_i} \tag{16}$$

The two sides of this equation are dimensionally equal (gas concentration $^{-1}$). Thus the difference between the two models is reduced to the idea that P&M can be described using bulk volumetric strain, multiplied by the inverse of a langmuir strain function and a constant determined from rock mechanical properties, whereas the ARI model employs matrix element shrinkage compressibility and the inverse slope of the isotherm as

measured from the initial desorption pressure. Note that these expressions would only be equivalent for saturated reservoir conditions and cases where the strain function is proportional to the isotherm function.

EXAMPLE

An example of the equivalence of the two methods is provided by substituting the P&M input and results from their large-scale San Juan basin evaluation into the ARI model. The basic parameters are listed in Table 1.

TABLE 1
INPUT PARAMETERS FOR MODEL COMPARISON

Φ, %	0.1,	0.5
E, psi	1.24E-05,	4.45E-05
υ	0.39	
M/E	2.0	
K/M	0.76	
γ, psi^{-1}	0	
$\beta = 1/P_l$, psi^{-1}	0.0016	
V_L , SCF/T (assumed)	500	
P_i, psi	1100	
ε_L/β	8	
$c_p = 1/2E\,\Phi$		

For this case, $\Phi_i = 0.001$, E= 445,000 psi and P= 0.0 psi (full depletion), the P&M model determines a change in porosity from 0.001 to 0.001724. For expressing change in permeability as a function of porosity, both models use

$$\frac{k}{k_i} = \left(\frac{\phi}{\phi_i}\right)^3 \qquad (17)$$

COMET software allows the value of the exponent to be selected by the user. This feature may be useful for particularly sensitive coals where an exponent higher than the normal default value of 3 may be necessary, as is apparently the case in some Australian coals. (Xavier Choi, CSIRO Australia, personal comm.)

Although the ratio of the porosity change is 1.7, due to the exponent in equation 17, the ratio of the permeability change by the P&M model is 5.12. Final permeability is more than five times greater than at initial conditions. The results of P&M's San Juan evaluation is summarized in their Figure 1 and is also reproduced here as Figure 1. Note that the permeability ratio of 5.12 represents the low-pressure endpoint of the appropriate curve in Figure 1.

This set of parameters is used to determine the value of matrix shrinkage compressibility, c_m, equal to 1.784E-06 psi^{-1}, which creates equivalence between the two models.** Results of the two models are then compared over a range of parameters for initial porosity, Young's modulus and pressure. Again, the P&M results are shown in Figure 1. Figure 2 shows that the comparable results from the ARI model are essentially identical.

In 1997, Mavor and Vaughn [9] described modeling increasing permeability in Valencia Canyon CBM wells in the San Juan Basin. They used the P&M model to calculate lookup tables of changing porosity and permeability that were then inserted into a reservoir simulator. They remarked that no prior reservoir model explained the behavior they observed. However, as one can conclude from the previous paragraph, *COMET* could have been used to arrive at essentially the same result.

UNDERSATURATED COALS

The previous example shows that the two models are equivalent for coals that are initially fully saturated with methane and the degree of swelling is directly proportional to methane concentration as defined by the isotherm. However, results appear to diverge if the coals are undersaturated. P&M uses rock mechanical properties and a continuous Langmuir-type strain vs. pressure relationship. Therefore, if reservoir pressure is reduced, matrix shrinkage is calculated to occur, regardless of gas concentration changes. When pressure is reduced in an undersaturated reservoir, pore compressibility effects act to reduce porosity and permeability, but no shrinkage will occur until gas desorbs and matrix gas concentration is reduced.

The ARI model directly employs the change in gas concentration to calculate shrinkage. If there is no change in concentration, as in early dewatering of an undersaturated reservoir, the model correctly calculates that there is no matrix shrinkage.

Consider the previous example, but with the data modified to describe an undersaturated reservoir, as in Table 2. Initial pressure remains 1,100 psi , but saturation pressure is now 800 psi.

TABLE 2
ADDITIONAL INPUT PARAMETERS FOR MODEL COMPARISON
(UNDERSATURATED RESERVOIR)

P_{sat}, psi	800
C_i, SCF/T	336.8

For this reservoir at 800 psi, the P&M model, determines a porosity of 0.000897, as shown in figure 3. Overall, porosity is reduced due to pore volume compressibility, but

** A value of c_m =1.784E-06 psi^{-1} compares favorably with the range of laboratory measurements of c_m, as summarized in Ref. No. 4

approximately two-thirds of the reduction has been incorrectly offset by shrinkage. The resulting permeability would be 72 percent of the original.

Applying these same parameters to the ARI model yields at 800 psi a porosity of 0.000663 and a corresponding permeability only 29 percent of the original. All of the porosity change is due to pore volume compressibility. No matrix shrinkage has occurred since no gas has yet been desorbed. This is consistent with work published by Gray [1]. At pressure below 800 psi, matrix shrinkage begins to have an effect, as shown by the ARI model. Eventually, at zero pressure, the two models converge. Both calculate the same maximum amount of porosity gain.

SWELLING NOT PROPORTIONAL TO GAS CONCENTRATION

Laboratory studies to date [4,5] have supported the observation that the amount of strain is approximately proportional to gas concentration. Langmuir gas concentration curves superimposed with Langmuir strain curves, as shown in Figure 4, illustrate this as a reasonable assumption, unless specific data to the contrary is known. The equivalence of the two shrinkage/swelling models, as discussed earlier, makes this assumption. However, if there is available laboratory data to show the strain function is substantially different than the gas concentration isotherm function, results of the two models will be different. If such a case is encountered, the P&M model can use the actual strain function (assuming the data can be fit to the Langmuir equation form) and would therefore be more accurate in predicting changes in porosity and permeability. The ARI model is limited to using the actual Langmuir adsorption isotherm. If the strain vs. pressure relationship does not follow the general form of the Langmuir equation, both models would be inaccurate in predicting porosity and permeability changes.

DIFFERENTIAL SWELLING

Levine [5] and others [2,4,6] have shown that exposing coal to CO_2 causes differing amounts of strain or permeability change compared to similar experiments using methane or helium, which is non-adsorptive. Much of this difference is attributable to the differing sorption capacity that any particular coal has for a particular gas. That is, the more gas adsorbed by a coal at a given pressure, the larger the effect on strain, porosity and permeability. Bustin [10] has recently investigated differing adsorptive capacities for a variety of gasses.

However, review of Levine's data reveals another mechanism is also at work. Replotting his data as volumetric strain vs. concentration (Matt Mavor, Tesseract Corp., personal comm.), as in Figure 5, shows that, on a unit concentration basis, CO_2 causes a greater degree of strain compared to CH_4. Porosity and permeability would be similarly affected. This observed difference is defined here as differential swelling. The authors make no comment on the physical or chemical basis for the existence of differential swelling, which may be an appropriate topic for additional academic and

laboratory research. The authors are not aware of additional data for other gasses, but believe it is reasonable to speculate that other gasses could each produce their own differential swelling effect. Such effects may cause more or less coal swelling, compared to CH_4.

Accounting for the impact of differential swelling in the reservoir would be an important consideration for numerical simulation of ECBM and CSEQ projects, both of which involve injecting significant volumes of CO_2. The practical implication of differential swelling is that injection of high pressure CO_2 may cause a greater degree of permeability loss than expected simply due to changes in in-situ gas concentration.

Based on this realization, differential swelling effects have been incorporated into the ARI model. This has been accomplished by inclusion of an additional term in equation 1. This new term is a differential swelling coefficient, c_k, which can be applied to the non-methane reservoir gas concentration.

$$\phi = \phi_i \left[1 - C_p(p - p_i) - c_m (1-\phi_i) \left(\frac{\Delta P_i}{\Delta C_i} \right) [(C - C_i) + c_k (C_t - C)] \right] \quad (18)$$

Through the addition of a differential swelling coefficient, *COMET* can effectively model the degree of matrix swelling based on the concentration of the injected gas and the amount of differential swelling the gas causes.

The differential swelling coefficient can be determined from laboratory isotherm and volumetric strain data. From Levine's data shown in Figure 5, c_k was determined to be 1.87. Use of this coefficient in equation 18 provides a very good replication of his CO_2 swelling data, as also shown in Figure 5.

The effects of the higher adsorptive capacity of CO_2, and differential swelling, on coal permeability are illustrated in Figure 6. This figure, which is based on similar conditions for methane as presented in Figures 1 and 2, demonstrates that both the higher adsorptive capacity of CO_2 (by approximately a factor of two) and a differential swelling coefficient of 1.87, combined can reduce coal permeability by over 80% from an initial value of 10 md at 1100 psi to less than 2 md.

FIELD EVIDENCE

Almost no field data exists for validating the laboratory findings and model predictions of coal swelling, with one notable exception. Since 1995 Burlington Resources has been injecting CO_2 into four wells in the Allison ECBM pilot in the San Juan basin. Data from those wells provides the only long-term, field-scale data to examine these phenomena.

Figure 7 presents the CO_2 injection rate and computed bottomhole pressure for one of those wells. Note that injection was performed at a relatively constant bottomhole pressure, and injection rate was permitted to vary. While injection has not been perfectly continuous, the long-term injectivity trends are clear. Initially, injectivity declined

significantly (from about 1.6 MMcfd at the start to a low of about 0.7 MMcfd approximately 12 months later). Subsequent to that period of declining injectivity, injectivity began a long period of improvement, which has continued through the last available data. These trends are consistent for all four of the injection wells, and hence are believed to be real indicators of reservoir behavior.

Pressure transient data from several producing wells in the field in the vicinity of the four injector wells had been collected in May, 2000. The results of their analysis suggested that in-situ coal permeability for the area was in the 100 – 130 md range. CO_2 contents of the produced gas from these wells was close to their initial levels, suggesting minimal, if any, influence of injected CO_2 on these permeability results. In August, 2001, the four injector wells were temporarily shut-in, and bottomhole pressure data collected. Results of analyzing these data suggested coal permeabilities in the <1 md range, two orders of magnitude less than the implied initial values, a reduction of 99%. These data provide our first insight into the potential magnitude of coal permeability reduction with CO_2 injection on a field-level basis, which are consistent with the ARI model predictions. Note that such a substantial permeability loss is not easily explained without considering differential swelling.

Using the ARI permeability function model, the permeability history of the injector wells was rationalized. This is illustrated in Figure 8. First, coal permeability at the injection well locations declined with a reduction in pore pressure. When the injection wells were drilled and injection commenced, a rapid reduction in permeability occurred as the CO2 saturated the injection area. Later in injection well history, the area became further depleted due to general reservoir pressure decline, leading to a continuous and gradual improvement in injectivity. This improvement would be expected to continue with time due to both depletion and matrix shrinkage effects. While somewhat subjective, this explanation is entirely consistent with field data, the results of reservoir simulation studies, and the predicted response based on the permeability function model presented in this paper.

CONCLUSIONS

For most CBM applications, the matrix shrinkage model presented by P&M in 1996 and 1998 provides results that are equivalent to the model developed by ARI in 1990.

The ARI model appears to more accurately handle undersaturated reservoirs.

The P&M model may be more accurate if a situation is encountered where matrix strain is only weakly proportional to gas concentration. However, both models may be inaccurate where strain is not proportional to gas concentration.

An existing body of data shows that matrix swelling and shrinkage of coals is an important factor in evaluating CBM reservoirs. However, this phenomenon is not yet fully described for a variety of gasses.

Differential swelling is a condition observed in laboratory data where CO_2 causes a different amount of volumetric strain, and by extension, a different degree of permeability change on a unit of concentration basis.

Differential swelling may also exist for other gasses, but laboratory and field studies have not yet been carried out to verify this.

The ARI model has been extended to replicate laboratory data of differential swelling. The application of this extension is demonstrated and supported by field behavior of CO_2 injection wells operating in the San Juan basin.

NOMENCLATURE

C	=	reservoir gas concentration, dimensionless
C_i	=	initial reservoir gas concentration, dimensionless
C_t	=	total reservoir gas concentration, dimensionless
c_k	=	differential swelling coefficient, dimensionless
c_m	=	matrix shrinkage compressibility, psi^{-1}
c_p	=	pore volume compressibility, psi^{-1}
Φ	=	fracture system porosity, decimal fraction
Φ_i	=	initial fracture system porosity, decimal fraction
E	=	Young's modulus, psi
f	=	decimal fraction, dimensionless
k	=	permeability, millidarcy
k_i	=	initial permeability, millidarcy
υ	=	Poisson's ratio
M	=	constrained axial modulus, psi
K	=	bulk modulus, psi
γ	=	grain compressibility, psi^{-1}
β	$= 1/P_L$ =	inverse of Langmuir pressure, psi^{-1}
ε_L	=	Langmuir strain, dimensionless
ε_m	=	bulk strain due to matrix swelling, dimensionless
S_m	=	matrix swelling coefficient, ton/scf
V_l	=	Langmuir volume, dimensionless
P_i	=	initial reservoir pore pressure, psi
P	=	reservoir pore pressure, psi
P_L	=	Langmuir pressure, psi

ACKNOWLEDGEMENT

The authors express their gratitude to the US Department of Energy, which provided funding for the research and preparation of this publication, cooperative Agreement No. DE-FC26-00NT-40924. We also thank Burlington Resources for permission to present their San Juan basin field data. We also acknowledge the helpful insights provided through personal communication with Xavier Choi of CSIRO Petroleum and Matt Mavor of Tesseract Corporation.

REFERENCES

1. Gray,I., Feb. 1987: “Reservoir Engineering in Coal Seams: Part I- The Physical Process of Gas Storage and Movement in Coal Seams”; SPERE, pp. 28-34.

2. Harpalani , S. and Schraufnagle, R. A., Sept. 1990: “Influence of Matrix Shrinkage and Compressibility on Gas Production from Coalbed Methane Reservoirs”, paper SPE 20729, Proceedings of the 65th Annual Technical Conference, New Orleans, LA.

3. Sawyer, W. K., Paul, G. W., and Schraufnagle, R. A., June 1990: “Development and Application of a 3D Coalbed Simulator”, paper CIM/SPE 90-119, Proceedings of the Petroleum Society CIM, Calgary.

4. Seidle, J.P. and Huitt, L. G., Nov. 1995: “Experimental Measurement of Coal Matrix Shrinkage Due to Gas Desorption and Implications for Cleat Permeability Increases”, paper SPE 30010, Proceedings of the International Meeting on Petroleum Engineering, Beijing, China, p. 575.

5. Levine, J. R., 1996: “Model Study of the Influence of Matrix Shrinkage on Absolute Permeability of Coal Bed Reservoirs”, in Gayer, R. and Harris, I. (eds), *Coalbed Methane and Coal Geology,* Geologic Society Special Publication. No. 109, pp. 197-212.

6. St. George, J. D. and Barakat, M. A., 2001: “The Change in Effective Stress with Shrinkage from Gas Desorption in Coal,” International Journal of Coal Geology, Vol. 45, pp. 105-113.

7. Palmer, I. and Mansoori, J., Oct. 1996: “How Permeability Depends on Stress and Pore Pressure in Coalbeds: A New Model,” paper SPE 36737, Proceedings of the 71st Annual Technical Conference, Denver, CO.

8. Palmer, I. and Mansoori, J., Dec. 1998: “How Permeability Depends on Stress and Pore Pressure in Coalbeds: A New Model,” paper SPE 52607, SPEREE, pp. 539-544.

9. Mavor, M. J. and Vaughn, J. E., May 1997: “Increasing Absolute Permeability in the San Juan Basin Fruitland Formation,” paper 9738, Proceeding of the International Coalbed Methane Symposium, University of Alabama/Tuscaloosa, pp.33-45.

10. Bustin, M. Mar. 2002: “Research Activities on CO_2, H_2S and SO_2 Sequestration at UBC,” presentation delivered at the Coal Sequestration I Forum, US Dept. of Energy, Houston, TX.

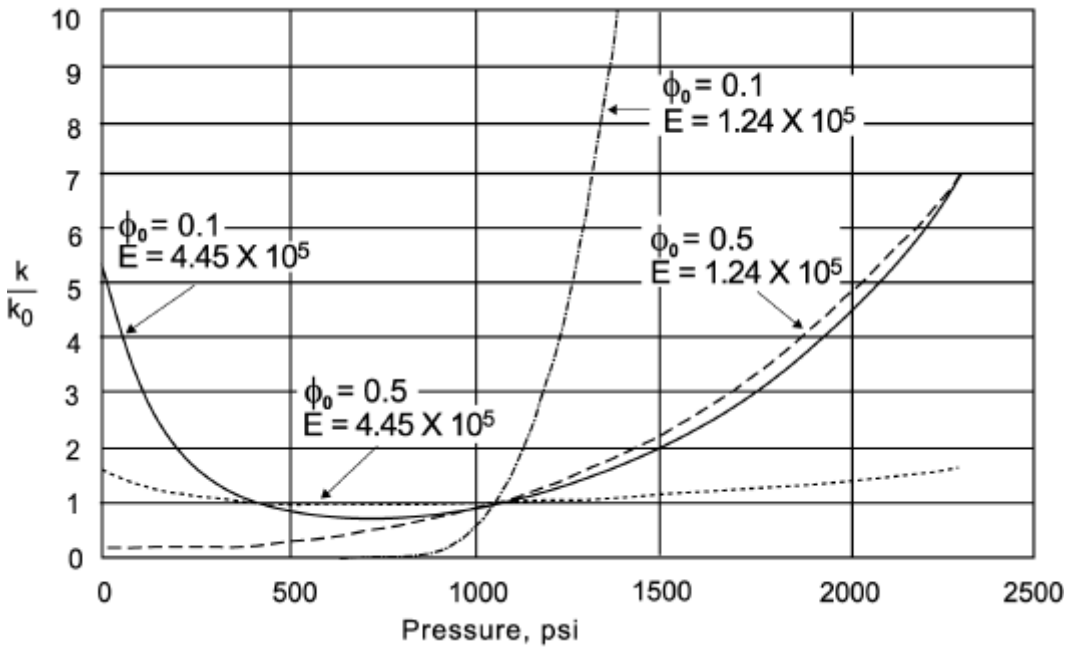

Figure 1. Variation in coal permeability with pressure. Results of Palmer and Mansoori model. Reproduced from SPE 36737.

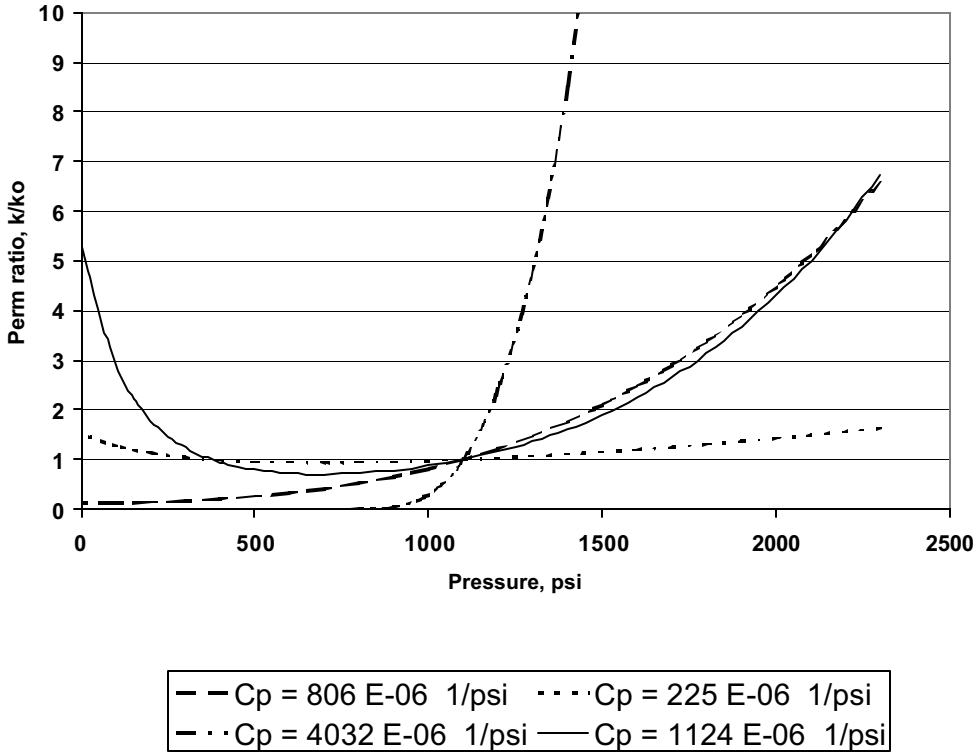

Figure 2. Variation of coal permeability ratio with pressure. Results of ARI model.

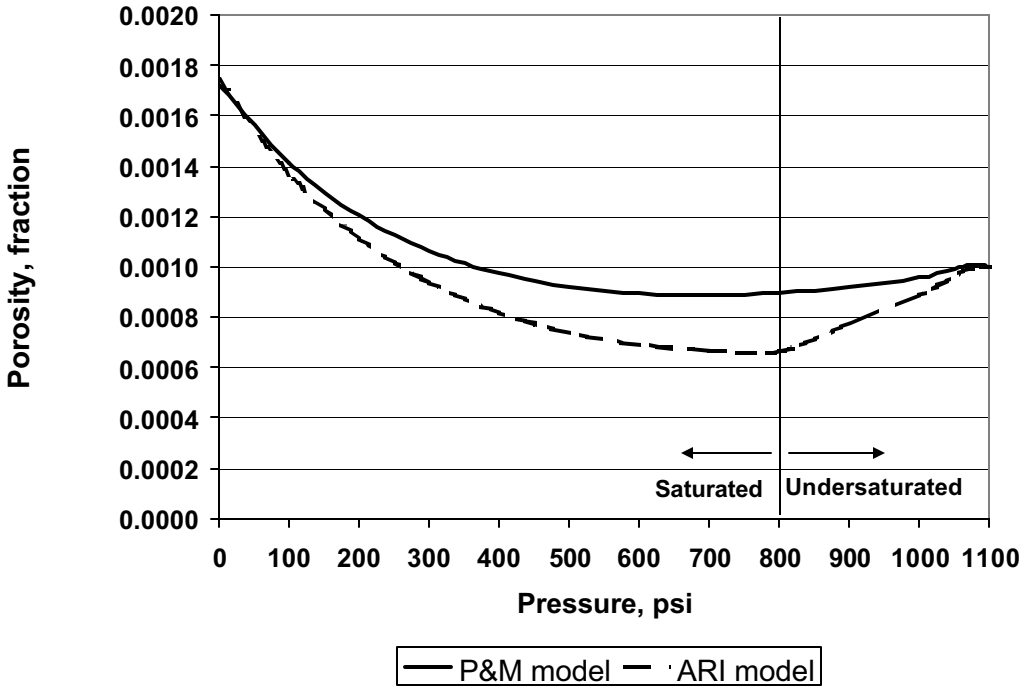

Figure 3. Variation in coal porosity with pressure. Undersaturated reservoir. ARI and P&M models.

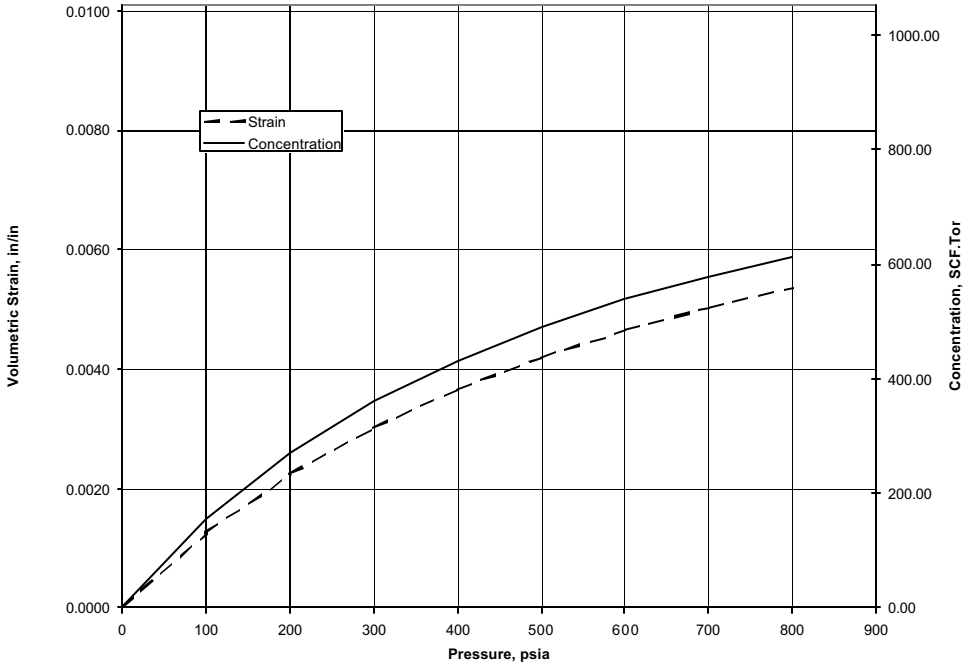

Figure 4. Volumetric strain and methane concentration vs. pressure. Data of Levine, Ref. 5. Strain axis range 0.0 to EL (0.0101); Concentration axis range 0.0 to VL (1053).

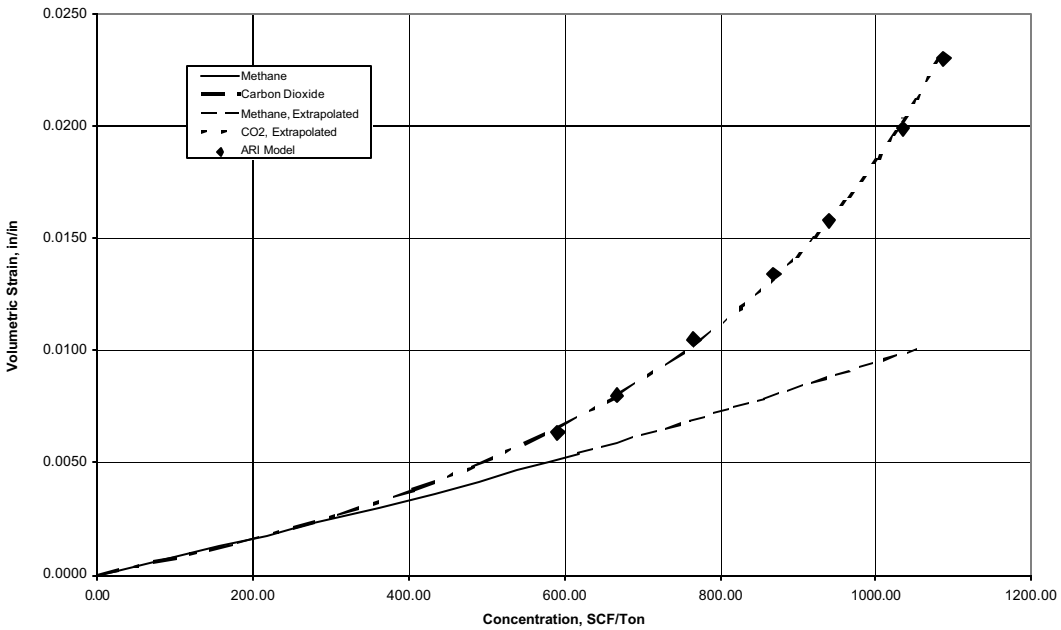

Figure 5. Volumetric strain vs. gas concentration for methane and carbon dioxide. Data replotted from Levine. ARI extended model for CO2 also shown using ck= 1.87

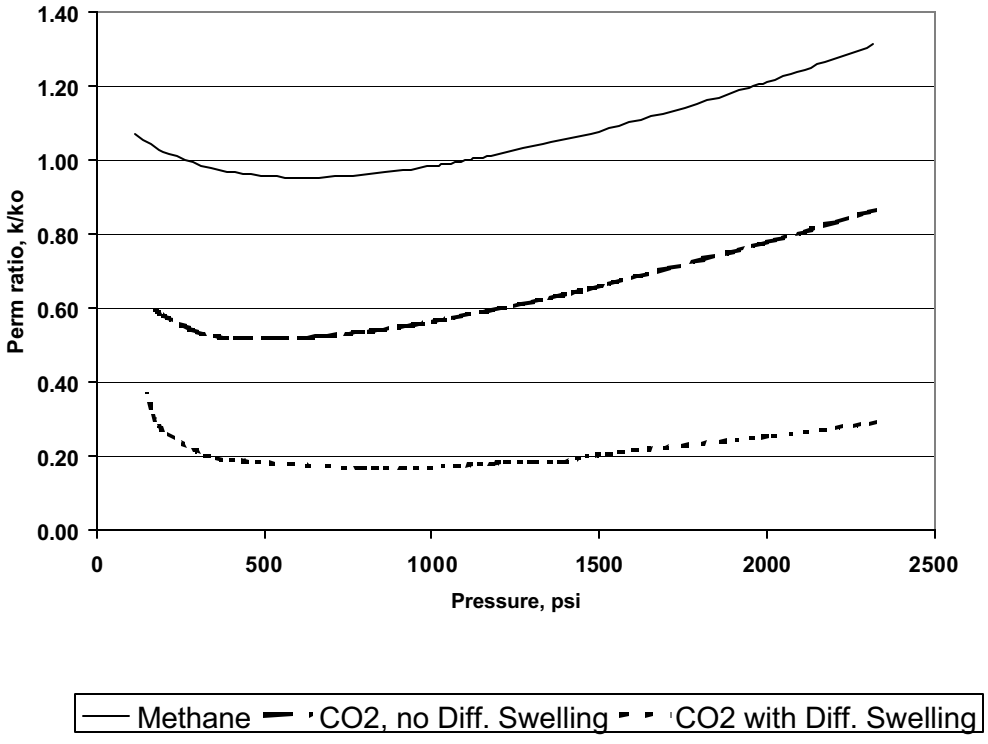

Fig.6 - Variation in ratio of coal permeability with pressure. Effect of CO2 with and without differential swelling.

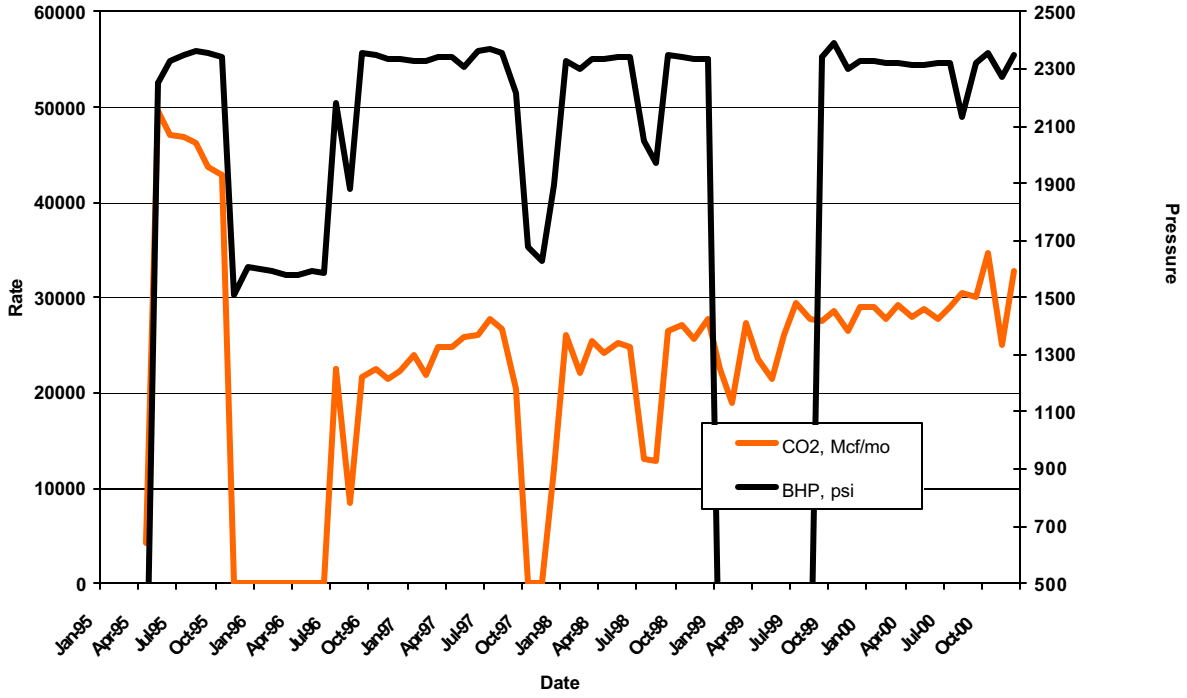

Figure 7: Injection/Pressure History for CO_2 Injection Well, Allison Unit, San Juan Basin

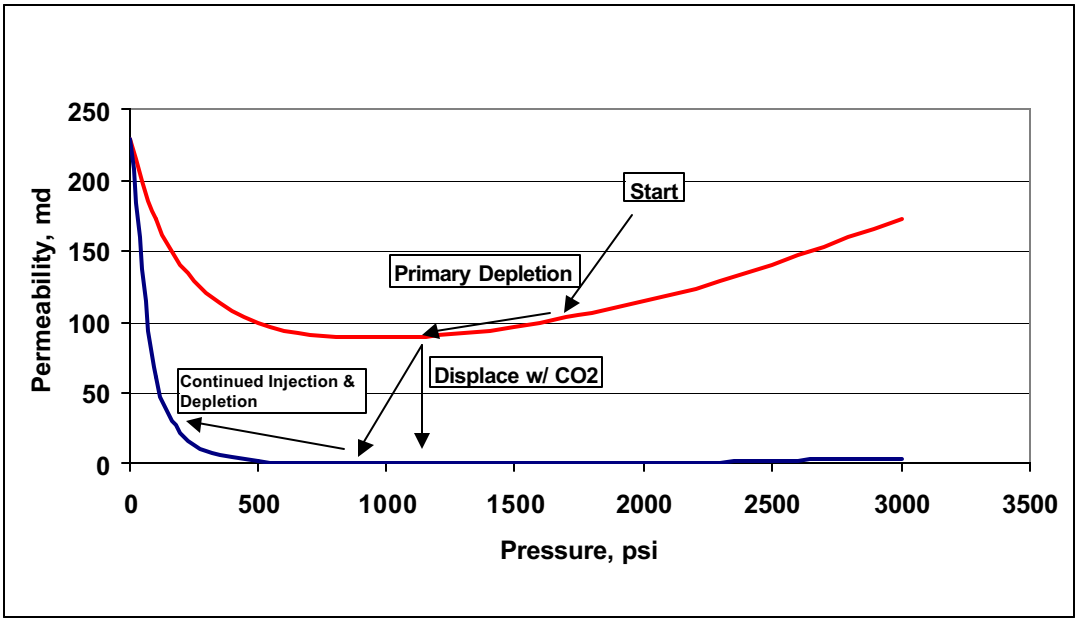

Figure 8: Permeability History for CO_2 Injection Well